
nnMOBILE-NET: RETHINKING CNN DESIGN FOR DEEP LEARNING-BASED RETINOPATHY RESEARCH

Wenhui Zhu

School of Computing and Augmented Intelligence
Arizona State University
AZ 85281, USA
wzhu59@asu.edu

Peijie Qiu*

McKeley School of Engineering
Washington University in St. Louis
St. Louis, MO 63130, USA

Natasha Lepore

CIBORG Lab
Department of Radiology Children's Hospital Los Angeles
Los Angeles, CA 90027, USA

Oana M. Dumitrascu

Department of Neurology
Mayo Clinic
Scottsdale, AZ 85251, USA

Yalin Wang

School of Computing and Augmented Intelligence
Arizona State University
AZ 85281, USA

ABSTRACT

Retinal diseases (RD) are the leading cause of severe vision loss or blindness. Deep learning-based automated tools play an indispensable role in assisting clinicians in diagnosing and monitoring RD in modern medicine. Recently, an increasing number of works in this field have taken advantage of Vision Transformer to achieve state-of-the-art performance with more parameters and higher model complexity compared to Convolutional Neural Networks (CNNs). Such sophisticated and task-specific model designs, however, are prone to be overfitting and hinder their generalizability. In this work, we argue that a channel-aware and well-calibrated CNN model may overcome these problems. To this end, we empirically studied CNN's macro and micro designs and its training strategies. Based on the investigation, we proposed a no-new-MobileNet (nn-MobileNet) developed for retinal diseases. In our experiments, our generic, simple and efficient model superseded most current state-of-the-art methods on four public datasets for multiple tasks, including diabetic retinopathy grading, fundus multi-disease detection, and diabetic macular edema classification. Our work may provide novel insights into deep learning architecture design and advance retinopathy research.

Keywords Retinal Diseases · Fundus image · Classification · CNN · Diabetic Retinopathy grading · Training tricks · MobileNet · Benchmark

1 Introduction

Retinal diseases (RD), including diabetic retinopathy (DR), age-related macular degeneration, inherited retinal conditions, and retinopathy of prematurity, are leading causes of blindness globally [1]. The automated RD diagnosis framework is crucial in modern medicine to guide the proper treatment of patients. In the past decade, deep learning has achieved state-of-the-art performance in automating the diagnosis of various RD. Following that trend, convolutional

*The authors contribute equally to this paper

neural networks (CNNs) [2, 3, 4, 5, 6, 7, 8] were dominating the early stages of development. Many studies have incorporated prior knowledge of the retinal lesion or the clinician-provided diagnosis into CNNs. Zoom-in-Net [3] took a biomimetic approach that used image magnification to locate lesions in the diagnosis of RD. Zhou et al. proposed a semi-supervised learning framework [4], which coordinated lesion segmentation and classification tasks by feature integrations. CANet [2] integrated two attention modules to jointly generate disease-specific and disease-dependent features for grading DR and diabetic macular edema (DME). Che et al. [7] achieved good performance via robust disentangled features of DR/DME. While these methods have demonstrated promising results, their complex and task-specific model designs were easy to overfit and required specific datasets (e.g., multi-task datasets).

Vision Transformers (ViT) have recently gained much attention in various visual tasks by leveraging the self-attention mechanism to capture long-term feature dependencies. Along this direction, MIL-VT [9] proposed using multiple-instance pooling to aggregate the features extracted by a ViT. Sun et al. [10] proposed a lesion-aware transformer (LAT) to learn the diabetic lesion-specific features via a cross-attention mechanism. To reduce the model complexity of transformer-based methods, Jiang et al. [11] proposed an efficient transformer design (SatFormer) by taking advantage of an efficient abnormality-aware attention mechanism and a saliency enhancement module for DR grading. Although those methods achieved state-of-the-art performance, most of them heavily relied on pretraining on large-scale datasets due to the data-hungry nature of ViT whose complexity quadratically grew with respect to the input size. In addition, the RD features are localized in nature. It was challenging for pure transformer-based feature extractors that more focused on global representations. To mitigate this issue, recent ViT advances [12, 13] converged to CNNs on bringing back convolutional operations. This motivated us to rethink the role of CNN in designing RD diagnostic models.

In this work, we rethought the issue of overfitting and frequently overlooked channel-wise information in RD classification tasks. For example, the radiation physical model of fundus images has been studied by Preece and Delori et al. [14, 15]. Light entering the inner eye was reflected, absorbed, and transmitted depending on tissue properties and pigment concentration. As a result, prime light colors, such as red, blue, and green colors, behaved differently in the fundus images. We hypothesized that radiation physics-aware channel-wise designs might benefit RD research. Our study also explored other key components of CNN architecture and its training strategies, including activation functions, spatial dropout, data augmentations, and optimizers. Based on our investigation, we proposed a fine-tuned lightweight CNN equipped with channel-information and studied its performance in a variety of retinal image datasets. The contribution of this paper can be summarized into four aspects. Firstly, we provided a new perspective on applying deep learning to fundus images. The high sensitivity of color fundus images to the channel was considered prior knowledge that can be incorporated into the model design. Secondly, we addressed a common overfitting issue in fundus image classification tasks by introducing dropout modules based on channel-wise information and combining heavy data augmentation. In particular, our study presented a counterintuitive result that heavy data augmentation helped improve performance, unlike the prevailing belief that heavy data augmentation disrupted the structure of medical images. Thirdly, based on our investigation, we proposed a series of modifications to MobileNetv2 [16] that demonstrated remarkable improvements in the classification of retinal diseases. Our method did not rely on complex multitasking but instead inherited its simple and efficient characteristics. Fourthly, our extensive experiments demonstrated that our work outperformed most state-of-the-art methods for various retinal disease tasks on multiple benchmark datasets. Overall, our study proposed a non-new network structure but rather fine-tuning an existing model based on the physical model and overfitting reduction schemes. We hope the new results presented in this study will provide novel perspectives on CNN design and encourage rethinking the importance of data essence and overfitting.

2 Methods

Guided by the hypothesis that channel-wise information played a crucial role in improving diagnostic performance for RD, our CNN architecture upon MobileNetv2 [16] used deepwise convolution and channel attention in each residual building block. We also empirically investigated optimizing the number of channels and incorporating Dropout in each residual building block to enhance the generalizability and prevent overfitting. To further address the overfitting problem, we adopted a heavy data-augmentation approach. Additionally, we explored the activation and optimizer to further improve the performance.

2.1 Network Design

Inverted linear residual block (ILRB): The original residual building block followed a trend of sequentially widening, narrowing, and finally widening the number of channels. Many modern designs of CNNs [17, 18, 16], however, inverted this order with a narrow to wide to narrow channel configuration by taking advantage of deep-wise convolution, namely inverted residual block (IRB). By further discarding the activation function after the last convolutional layer to prevent information loss during the rectified linear unit (ReLU) activation, the IRB turned to an inverted linear

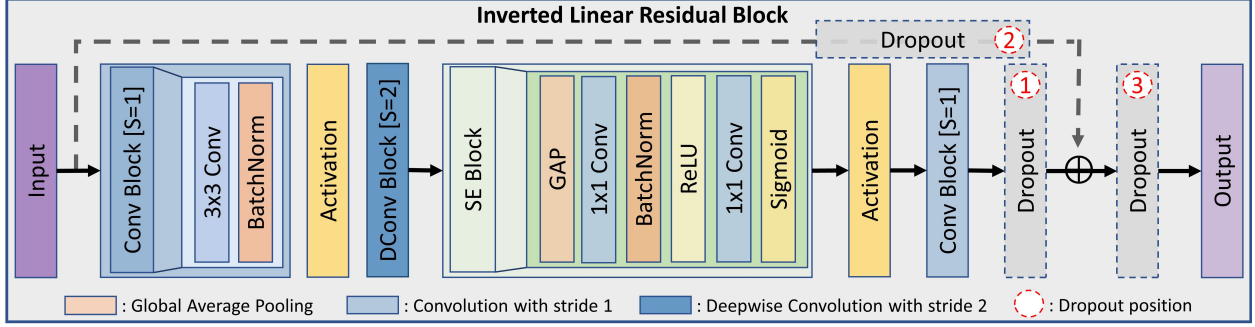


Figure 1: Inverted linear residual block (ILRB) architecture design.

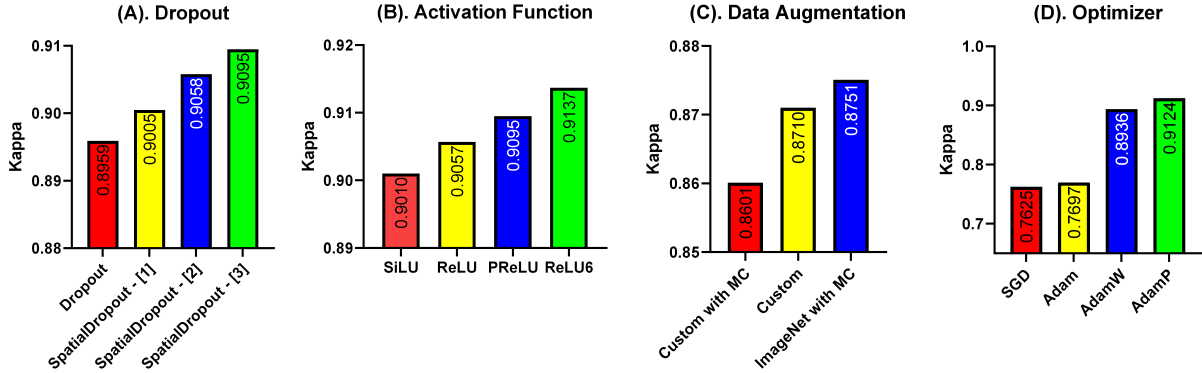


Figure 2: Empirical parameter study results Based on Messidor-2 dataset [21]. Subpanel pictures (a), (b), (c), and (d) represent different experimental groups, each of which was independent of the others. We kept the other parameters consistent in each experiment, but it did not mean the other parameters were the best. MC denotes Mixup[22] and CutMix[23], and SDropout-[x] denotes placed SpatialDropout in position x as shown in Fig. 1.

residual block (ILRB). The deepwise convolution performed separate 2D convolution on a per-channel basis and then weighted the feature map of each channel by a 1×1 convolution to aggregate the channel dimension, which resembled the Convolutional Block Attention Module in [19]. To further capture the channel-wise information, the Squeeze-and-Excitation block in [20] was adopted to each residual block. We kept the same stem setting (i.e., channel configuration and the number of filters) of each ILRB as that in [17] with an expansion rate of 1 for the first ILRB and 6 otherwise. The expansion rate denotes the rate of channel dimensions between the hidden layers and the input to each ILRB module. Fig. 1 shows the detailed structure of the ILRB module. The effectiveness of this module was also demonstrated in subsequent ablation experiments.

Activation Function (AF): Recently, Han et al. [17] uncovered the effect of complicated nonlinear activation functions (e.g., ELU or SiLU) in visual tasks by leveraging that the matrix rank of the output feature can estimate the expressiveness of a layer. Although surprising performance has been achieved when applied in natural images where the region of interest is always well-defined, it is likely to be problematic when directly translating to retinal fundus images where tiny and hardly distinguishable lesions (e.g., Microaneurysms) are of most interest. Inspired by this observation, We conducted empirical studies of the impact of different activation functions (i.e., SiLU, ReLU, PReLU, ReLU6) on RD tasks. As shown in Fig. 2(B), the ReLU6 activation was the best among all options.

Dropout (D): Most RD diagnostic models suffer from the issue of overfitting mainly due to the heterogeneous appearance of pathological biomarkers in terms of size, shape, and location. For example, DR diagnostic models are always struggling to classify Microaneurysms. Dropout is widely used to mitigate overfitting and improve generalizability. But where and how to place Dropouts remain an open question. In this study, we tried to answer this question by investigating two common dropout modes and their positions in the network. The first one was the regular random dropout which randomly zeroed out entries in the feature map following a Bernoulli distribution. The second mode was spatial-dropout [24] (channel-wise dropout) that randomly zeroed out channels in the feature map, which

matched our previous hypothesis on channel-wise information. We investigated three possible locations of Dropout placement in the ILRB (Fig. 1) where location 3 showed the best performance (Fig. 2(A)).

2.2 Training Techniques

Data Augmentations (DA): Most previous work [10, 11, 2, 9] held the view that excessive data augmentation could potentially compromise the integrity of fundus data. Therefore, data augmentations including spatial transformations and brightness adjustments were always recommended in retinal fundus images. Nevertheless, these data augmentations could not eliminate overfitting in the RD tasks based on our empirical studies. Building upon the aforementioned observations, exploratory experiments were conducted to optimize the data augmentation strategies that better prevent overfitting. We presented three data augmentation combinations: (I). Customized data augmentations in methods [10, 11]; (II). Customized data augmentations in methods [10, 11] with Mixup [22] and CutMix [23]; (III). The official ImageNet data augmentation techniques [18] (e.g., RandAugment[25] and Random Erasing[26]) with Mixup and CutMix. Our empirical studies showed that the heaviest data augmentations (III) led to the best performance (Fig. 2(C)). Our software package is available at <https://github.com/Retinal-Research/NNMOBILE-NET>.

Optimizer (O): Recent empirical studies demonstrated that performance improvement was gained by training the neural networks with more advanced optimizers (e.g., AdamW [27], AdamP [28]) that better accommodated the step size adaptively. As shown in Fig. 2(D), our empirical studies showed that training the network with AdamP optimizers significantly increased the performance.

3 Experiments and Results

An optimal set of network structures and training strategies is summarized in Section 2. We used cross-entropy loss for training all the models in this work. The initial learning rate was set to 0.001 decayed according to a cosine decay learning rate scheduler with 20 epochs of linear warm-up. A weight decay rate of 0.05 was applied to prevent further overfitting. All experiments were performed on three GeForce RTX 3090 with a batch size of 32 and 1000 epochs. All were implemented in PyTorch. Experimental results are summarized in Tables 1 to 5.

3.1 Datasets and Evaluation Metrics

Messidor-1 dataset [21] contains 1200 fundus images with four DR grades. We conducted referral and normal DR classification in this dataset. In the referral and non-referral DR classification, Grades 0 and 1 are considered non-referable, while Grades 2 and 3 are considered referable DR (rDR). For normal and abnormal classification, only Grade 0 will be labeled as normal, and the other grades are recognized as abnormal. We followed the experimental settings in [2] by using 10-fold cross-validation on the entire dataset. The area under the curve (AUC) was used as the evaluation metric. **Messidor-2 dataset** [21] contains 1748 fundus images with five DR grades. As no official split of the training and testing dataset was provided, we used this dataset to conduct ablation studies to demonstrate the effectiveness of each component of our proposed method on DR grading evaluated by the AUC and quadratic cohen’s kappa (Kappa). **RFMiD dataset** [29] contains 1920 training, 640 validation, and 640 testing images with 45 different types of pathologies (central serous retinopathy, central retinal vein occlusion, asteroid hyalosis, etc.). Following the protocol in [11, 9], we performed normal and abnormal binary classification on this dataset whose performance is measured by accuracy (ACC), AUC, and F1. **APOTS dataset** [30] contains 3662 fundus images for DR grading with the severity on a grade of 0 to 4 (no DR, mild, moderate, severe, proliferative DR). Following the experimental setting of 5-fold cross-validation in [9], we evaluated the performance of DR grading in terms of ACC, AUC, weighted F1, and kappa. **IDRiD dataset** [31] contains 413 training and 103 testing images for both DR grading and DME severity grading tasks. we used the training and testing data provided by the official split. Different from method [2] that re-labeled DR grading into two categories, we trained the multi-class DR grading task and reported the evaluation metrics of ACC, AUC, and F1. Both grading experiments followed the protocol in [7].

3.2 Ablation Studies

To quantify the importance of each proposed module in Section 2, we performed a series of ablation studies on the DR grading task on the Messidor-2 dataset. Table 1 reports the results of all the ablation studies. We found that applying heavy data augmentations (DA) during training had the highest performance gain increasing the AUC and Kappa by 3.06% and 2.71%, respectively². Meanwhile, the ILRB module also significantly improved the performance of the DR grading by 2.22% in the AUC and 1.53% in the Kappa. Besides, the ReLU6 activation function, spatial dropout, and

²The performance gain was calculated as $\frac{(\text{Final Value} - \text{Baseline Value})}{\text{Baseline Value}} \times 100\%$.

Table 1: Ablation Studies on the DR grading task on the Messidor-2 dataset [21]. ResNet-50 [32] served as the comparison model in the initial line.

ILRB	DA	D	O	AF	AUC	Kappa
X	X	X	X	X	91.19	85.76
✓	X	X	X	X	93.22	87.06
✓	✓	X	X	X	96.08	89.42
✓	✓	✓	X	X	96.14	90.58
✓	✓	✓	✓	X	96.13	90.72
✓	✓	✓	✓	✓	96.52	91.37

Table 2: Comparison of rDR and normal classification on the Messidor-1 dataset [21]. Annotations denote whether pixel-level or patch-level supervision was applied.

Method	Annotations	Referral AUC	Normal AUC
VNXX [33]	-	88.7	87.0
CKML [33]	-	89.1	86.2
Comp. CAD [6]	-	91.0	87.6
Expert A [6]	-	94.0	92.2
Expert B [6]	-	92.0	86.5
Zoom-in-Net [3]	-	95.7	92.1
AFN [5]	patch	96.8	-
Semi + Adv [4]	pixel	97.6	94.3
CANet[2]	-	96.3	-
LAT [10]	-	98.7	96.3
Ours	-	98.7	97.5

AdamP optimizer together contributed to a performance gain of 0.48% in AUC and 2.2% in the Kappa. Even though there was only a minor increase in the AUC, the Kappa, which measured the grading accuracy, increased dramatically, especially after applying the spatial dropout (Table 1). With all proposed modifications, we drove the AUC from 91.19 to 96.52 (6.15%) and the Kappa from 85.76 to 91.37 (6.5%). Based on our ablation study results, the factors which led to a significant performance improvement were revealed. Among them, the common overfitting reduction schemes (data augmentation and spatial dropout) contributed the most, followed by the ILRB module guided by channel-wise information.

3.3 Comparison to State-Of-The-Art Methods

DR task performance. We compared the proposed method to a variety of existing state-of-the-art (SOTA) methods on three DR datasets (i.e., Messidor1, APOTS, and IDRID). The proposed method achieved the best performance on the IDRID dataset (AUC=91.6, ACC=73.1). Remarkably, the proposed method outperformed the best model (DETACH-DAW [7]) by 8% and 23.5% in AUC and ACC (Table 5), respectively, on the IDRID dataset. We also found that the proposed method had the highest ACC and Kappa on the APOTS dataset with a similar AUC to the best-performed model (Table 4). The proposed method achieved an equal performance to the best model (LAT [10]) on the referral DR classification task and the best performance on the normal DR classification task (Table 2). It is worth noting that most works (i.e., MIL-VT [9], LAT [10], Zoom-in-Net [3], Semi + Adv [4], and CKML [33]) were pre-trained on large-scale external datasets. Whereas, the proposed method was trained from scratch using the same benchmark datasets.

Multi-disease abnormal detection performance. We also conducted experiments and comparisons to current SOTA methods on the multi-disease detection task. The proposed method achieved the best performance in terms of ACC and AUC, while the SatFormer-B [11] achieved the best performance in F1 (Table 3). However, our model (Param=34M) has fewer than half number of parameters of the SatFormer-B [11] (Param=78M). Even though the proposed model had a similar stem architecture to the RexNet, our heavy data augmentations and spatial dropout improved the ACC by 3.4% and AUC by 4.4%.

Table 3: Performance comparison of multi-disease abnormal detection on the RFMiD dataset [29]. Param are the parameter numbers, indicating model complexity of models.

Method	Param(M)	Normal/Abnormal		
		ACC	AUC	F1
CANet[2]	29	88.3	91.0	90.4
EffNet-B7[34]	66	88.2	91.0	90.7
ReXNet[17]	34	91.3	94.5	93.3
CrossFormer-L[35]	92	90.6	94.3	92.0
Swin-L[36]	197	89.5	93.8	91.6
MIL-VT[9]	98	91.1	95.9	94.4
SatFormer-B [11]	78	93.8	96.5	95.8
Ours	34	94.4	98.7	94.4

Table 4: Performance comparison of DR grading on the APOTS dataset [30].

Method	DR Grading			
	AUC	ACC	F1	Kappa
DLI[37]	-	82.5	80.3	89.0
CANet[2]	-	83.2	81.3	90.0
GREEN-ResNet50 [38]	-	84.4	83.6	90.8
GREEN-SE-ResNext50 [38]	-	85.7	85.2	91.2
MIL-VT [9]	97.9	85.5	85.3	92.0
Ours	97.8	89.1	88.9	93.4

Table 5: Performance comparison of DR and DME grading on the IDRID dataset [31].

Method	DME			DR		
	AUC	F1	ACC	AUC	F1	ACC
CANet[2]	87.9	66.1	78.6	78.9	42.3	57.3
Multi-task net[39]	86.1	60.3	74.8	78	43.9	59.2
MTMR-net[40]	84.2	61.1	79.6	79.7	45.3	60.2
DETACH + DAW [7]	89.5	72.3	82.5	84.8	49.4	59.2
Ours	95.3	84.8	86.5	91.6	72.6	73.1

DME classification performance. The DME classification task was evaluated on the IDRID dataset following the protocol in [7]. Table 5 demonstrated that the proposed method surpassed the model with the best performance (DETACH+DAW [7]) by 17.3% on F1, 6.5% on AUC, and 4.8% on ACC. Compared to other SOTA methods (i.e., CANet [2], Multi-task net [39], MTMR-net [40], and DETACH-DAW [7]) that were jointly trained on multiple tasks, our proposed model was trained from scratch on the DME task only.

4 Conclusion

In this paper, we provided novel insights into the RD diagnostic model design informed by the channel-wise information in retinal fundus images. A generic and efficient CNN-based architecture design and its training strategies were proposed for general RD tasks. Our comprehensive experimental results demonstrated that a properly tuned CNN rather than a model with a huge number of parameters and complex structures could compete favorably with current SOTA methods across multiple RD tasks on benchmark datasets.

Acknowledgement. This work was partially supported by grants from NIH (R21AG065942, R01EY032125, and R01DE030286), and the State of Arizona via the Arizona Alzheimer Consortium.

References

- [1] David Yorston. Retinal diseases and vision 2020. *Community Eye Health*, 16(46):19–20, 2003.
- [2] X. Li, X. Hu, L. Yu, L. Zhu, C. W. Fu, and P. A. Heng. CANet: Cross-Disease Attention Network for Joint Diabetic Retinopathy and Diabetic Macular Edema Grading. *IEEE Trans Med Imaging*, pages 1483–1493, 2020.
- [3] Zhe Wang, Yanxin Yin, Jianping Shi, Wei Fang, Hongsheng Li, and Xiaogang Wang. Zoom-in-net: Deep mining lesions for diabetic retinopathy detection. In *MICCAI*, pages 267–275, 2017.
- [4] Yi Zhou, Xiaodong He, Lei Huang, Li Liu, Fan Zhu, Shanshan Cui, and Ling Shao. Collaborative learning of semi-supervised segmentation and classification for medical images. In *Proc. IEEE Comput. Soc. Conf. Comput. Vis. Pat- tern Recognit*, 2019.
- [5] Zhiwen Lin, Ruoqian Guo, Yanjie Wang, Bian Wu, Tingting Chen, Wenzhe Wang, Danny Z. Chen, and Jian Wu. A framework for identifying diabetic retinopathy based on anti-noise detection and attention-based fusion. In *MICCAI*, pages 74–82, Cham, 2018. Springer.
- [6] Clara I Sánchez and et al. Evaluation of a computer-aided diagnosis system for diabetic retinopathy screening on public data. *Investigative ophthalmology & visual science*, 52(7):4866–4871, 2011.
- [7] Haoxuan Che, Haibo Jin, and Hao Chen. Learning robust representation for joint grading of ophthalmic diseases via adaptive curriculum and feature disentanglement. In *MICCAI*, pages 523–533, 2022.
- [8] Wenhui Zhu and et al. Self-supervised equivariant regularization reconciles multiple instance learning: Joint referable diabetic retinopathy classification and lesion segmentation. *18th International Symposium on Medical Information Processing and Analysis (SIPAIM)*, 2022.
- [9] Shuang Yu and et al. Mil-vt: Multiple instance learning enhanced vision transformer for fundus image classification. In *MICCAI*, pages 45–54. Springer, 2021.
- [10] Rui Sun, Yihao Li, Tianzhu Zhang, Zhendong Mao, Feng Wu, and Yongdong Zhang. Lesion-aware transformers for diabetic retinopathy grading. In *Proc. IEEE Comput. Soc. Conf. Comput. Vis. Pat- tern Recognit*, pages 10938–10947, 2021.
- [11] Yankai Jiang and et al. Satformer: Saliency-guided abnormality-aware transformer for retinal disease classification in fundus image. In *Proceedings of the Thirty-First International Joint Conference on Artificial Intelligence, IJCAI*, pages 987–994, 2022.
- [12] Ze Liu and et al. Swin transformer: Hierarchical vision transformer using shifted windows. In *Proc. IEEE Int. Conf. Comput. Vis.(ICCV)*, pages 10012–10022, 2021.
- [13] Prajit Ramachandran, Niki Parmar, Ashish Vaswani, Irwan Bello, Anselm Levskaya, and Jon Shlens. Stand-alone self-attention in vision models. *Advances in neural information processing systems*, 32, 2019.
- [14] Stephen J Preece and Ela Claridge. Monte carlo modelling of the spectral reflectance of the human eye. *Physics in Medicine & Biology*, 47(16):2863, 2002.
- [15] François C Delori and Kent P Pflibsen. Spectral reflectance of the human ocular fundus. *Applied optics*, 28(6):1061–1077, 1989.
- [16] Mark Sandler, Andrew Howard, Menglong Zhu, Andrey Zhmoginov, and Liang-Chieh Chen. Mobilenetv2: Inverted residuals and linear bottlenecks. In *Proc. IEEE Comput. Soc. Conf. Comput. Vis. Pat- tern Recognit*, pages 4510–4520, 2018.
- [17] Dongyoon Han, Sangdoo Yun, Byeongho Heo, and YoungJoon Yoo. Rethinking channel dimensions for efficient model design. In *Proceedings of the IEEE/CVF conference on Computer Vision and Pattern Recognition*, pages 732–741, 2021.
- [18] Zhuang Liu, Hanzi Mao, Chao-Yuan Wu, Christoph Feichtenhofer, Trevor Darrell, and Saining Xie. A convnet for the 2020s. In *Proc. IEEE Comput. Soc. Conf. Comput. Vis. Pat- tern Recognit*, pages 11976–11986, 2022.
- [19] Sanghyun Woo, Jongchan Park, Joon-Young Lee, and In So Kweon. Cbam: Convolutional block attention module. In *Comput Vis ECCV*, pages 3–19, 2018.
- [20] Jie Hu, Li Shen, and Gang Sun. Squeeze-and-excitation networks. In *Proceedings of the IEEE conference on computer vision and pattern recognition*, pages 7132–7141, 2018.
- [21] Etienne Decencière and et al. Feedback on a publicly distributed image database: The messidor database. *Image Analysis & Stereology*, 2014.
- [22] Hongyi Zhang, Moustapha Cisse, Yann N. Dauphin, and David Lopez-Paz. mixup: Beyond empirical risk minimization. In *International Conference on Learning Representations*, 2018.

- [23] Sangdoo Yun, Dongyoon Han, Seong Joon Oh, Sanghyuk Chun, Junsuk Choe, and Youngjoon Yoo. Cutmix: Regularization strategy to train strong classifiers with localizable features. In *Proc. IEEE Int. Conf. Comput. Vis.(ICCV)*, pages 6023–6032, 2019.
- [24] Jonathan Tompson, Ross Goroshin, Arjun Jain, Yann LeCun, and Christoph Bregler. Efficient object localization using convolutional networks. In *Proceedings of the IEEE conference on computer vision and pattern recognition*, pages 648–656, 2015.
- [25] Ekin D Cubuk, Barret Zoph, and et al. Randaugment: Practical automated data augmentation with a reduced search space. In *Proceedings of the IEEE/CVF conference on computer vision and pattern recognition workshops*, pages 702–703, 2020.
- [26] Zhun Zhong and et al. Random erasing data augmentation. In *Proceedings of the AAAI conference on artificial intelligence*, volume 34, pages 13001–13008, 2020.
- [27] Ilya Loshchilov and Frank Hutter. Decoupled weight decay regularization. In *International Conference on Learning Representations*.
- [28] Byeongho Heo, Sanghyuk Chun, Seong Joon Oh, Dongyoon Han, Sangdoo Yun, Gyuwan Kim, Youngjung Uh, and Jung-Woo Ha. Adamp: Slowing down the slowdown for momentum optimizers on scale-invariant weights. *arXiv preprint arXiv:2006.08217*, 2020.
- [29] Samiksha Pachade and et al. Retinal fundus multi-disease image dataset (rfmid). 2020.
- [30] Aptos database.
- [31] Prasanna Porwal and et al. Indian diabetic retinopathy image dataset (idrid). 2018.
- [32] Kaiming He, Xiangyu Zhang, Shaoqing Ren, and Jian Sun. Deep residual learning for image recognition. In *Proceedings of the IEEE conference on computer vision and pattern recognition*, pages 770–778, 2016.
- [33] Holly H. Vo and Abhishek Verma. New deep neural nets for fine-grained diabetic retinopathy recognition on hybrid color space. In *2016 IEEE International Symposium on Multimedia (ISM)*, pages 209–215, 2016.
- [34] Mingxing Tan and Quoc Le. Efficientnet: Rethinking model scaling for convolutional neural networks. In *International conference on machine learning*. PMLR, 2019.
- [35] Wenxiao Wang, Lu Yao, Long Chen, Binbin Lin, Deng Cai, Xiaofei He, and Wei Liu. Crossformer: A versatile vision transformer hinging on cross-scale attention. *arXiv preprint arXiv:2108.00154*, 2021.
- [36] Yawei Li, Kai Zhang, Jiezhong Cao, Radu Timofte, and Luc Van Gool. Localvit: Bringing locality to vision transformers. *arXiv preprint arXiv:2104.05707*, 2021.
- [37] Alexander Rakhlin. Diabetic retinopathy detection through integration of deep learning classification framework. *BioRxiv*, page 225508, 2017.
- [38] Shaoteng Liu, Lijun Gong, Kai Ma, and Yefeng Zheng. Green: a graph residual re-ranking network for grading diabetic retinopathy. In *MICCAI*, pages 585–594, Cham, 2020. Springer International Publishing.
- [39] Q. Chen and et al. A multi-task deep learning model for the classification of Age-related Macular Degeneration. *AMIA Jt Summits Transl Sci Proc*, 2019.
- [40] L. Liu and et al. Multi-Task Deep Model With Margin Ranking Loss for Lung Nodule Analysis. *IEEE Trans Med Imaging*, 39(3):718–728, 2020.